Electrochimica Acta 206 (2016) 70–76

Contents lists available at ScienceDirect

Electrochimica Acta

journal homepage: www.elsevier.com/locate/electacta

The Effect of Pre-Analysis Washing on the Surface Film of Graphite Electrodes

L. Somerville[a,b], J. Bareño[a], P. Jennings[b], A. McGordon[b], C. Lyness[c], I. Bloom[a,*]

[a] Argonne National Laboratory, 9700 S. Cass Ave.; Lemont, IL 60561, USA
[b] WMG, University of Warwick, Coventry, England CV4 7AL, UK
[c] Jaguar Land Rover, Banbury Road, Warwick, England CV35 0XJ, UK

ARTICLE INFO

Article history:
Received 2 April 2016
Received in revised form 22 April 2016
Accepted 23 April 2016
Available online 25 April 2016

Keywords:
Lithium-ion
XPS
post-test analysis
SEM
battery lifetime prediction
infra-red spectroscopy

ABSTRACT

Electrodes are routinely washed to remove electrolyte deposits, salt, and high boiling point solvents prior to analysis with surface-sensitive techniques. The effect of washing on the surface films of graphite electrodes from $LiCoO_2$/graphite cells, which contained varying amounts of vinylene carbonate (VC), was investigated by comparing the microstructure and chemical composition. We confirmed that there are two different kinds of films on the surface of the electrodes: one at low and one at high VC content concentration. Far from being limited to remove extraneous salt deposits from the surface of the sample, DMC washing was found to completely remove one and to affect the composition of deeper strata in the other.

1. Introduction

Lithium-ion cells are the energy storage solution of choice in most handheld and portable electronics. However, the power and capacity of these cells can be reduced considerably dependent on storage and usage conditions [1]. For a mobile phone or a laptop computer, with short innovation cycles where it is replaced by a newer model every couple of years, this is not a significant problem. For cells used in vehicles and medical electronics, which are used for much longer (8+ years), battery degradation issues present considerable challenges in maintaining power and capacity over the cells' lifetimes [2].

A single lithium-ion cell consist of two electrodes separated by a permeable polymer membrane. Ion transport is facilitated between electrodes by the electrolyte. The negative electrode is most often graphite and the positive electrode lithiated metal oxide. The electrolyte usually consists of a mixture of organic carbonates and a lithium salt. Within the first few cycles of a lithium-ion cell, a film is formed at one [3] and perhaps both electrodes [4]. This film, a solid electrolyte interphase (SEI) [5] layer, passivates the electrode surface to further reaction with the components of the electrolyte [6]. The study and characterization of these films, to determine their chemical composition and properties, have been the subject of many years of research. The knowledge gained from these studies could lead to improvements in cell lifetime or performance.

Before characterizing the surface film, most authors wash the electrode with a low boiling point solvent. Lu et al. report that the reason for this is to remove higher boiling point electrolyte solvents [3]. Yang et al. report that, in addition to removing the electrolyte solvent, washing also removed residual salt which had been deposited onto the electrode after the more volatile electrolyte components had evaporated [4].

There is a distinct possibility that the washing process, which in some cases is quite prolonged [7], may affect the composition of the SEI or partially remove it. Dedryvère et al. used acetonitrile to remove PEO oligomers, Li_2CO_3 and CH_3OCO_2Li from the surface of stainless steel electrodes, allowing them to study the underside of the surface film [8]. Malmgren et al. rinsed electrodes with DMC and found that the sensitivity of the exposed graphite to air increased after the rinsing process [9]. They conclude that the increased sensitivity of electrodes to air shows that the rinsing process has removed the passivating surface film.

In addition, Williard et al. state that washing with solvent may lead to removal of SEI [10]. Whilst Orsini et al. state that washing is always the subject of controversy [11]. If analysis is performed on these washed (hence, possibly chemically changed) SEI films, the conclusions may be incorrect.

* Corresponding author. Tel.: +1 630 252 4516.
E-mail address: ira.bloom@anl.gov (I. Bloom).

http://dx.doi.org/10.1016/j.electacta.2016.04.133

In this paper, we report the effect that washing has on the SEI films of graphite electrodes from $LiCoO_2$/graphite cells that also contained small amounts of vinylene carbonate (VC). Vinylene carbonate is well known to have a positive effect on a cell's performance over its lifetime and this performance peaks somewhere between 1 and 2% [12]. The reason for this is due to a reaction at the negative electrode to change the composition of the surface film. VC is used because it helps to elucidate the effect that washing has on the electrodes.

To determine if washing only removes salt and solvent, we characterized the surface film of both washed and unwashed negative graphite electrodes using x-ray photoelectron spectroscopy (XPS), scanning electron microscopy (SEM), and attenuated total reflectance (ATR) Fourier transform infra-red (FTIR) spectroscopy.

2. Experimental

2.1. Materials

Aged, 300 mAh $LiCoO_2$/graphite pouch cells, containing 0, 1, 2, 4, and 6 vol. % VC, were used in this work. The electrolyte in these cells was 1 M $LiPF_6$ in ethylene carbonate (EC)/ethyl methyl carbonate (EMC), 3:7, by wt. They were cycled between 3.78 V and 4.2 V nine times over 12 days at a rate of C/10 and under ambient conditions.

The cells were then discharged to 0.5 V and dismantled in an argon-filled glove box. The cathode/separator/anode roll was unwound and samples were cut from the bulk of the electrode material using stainless steel scissors. Care was taken to handle the samples with tweezers by the edges. Half of the electrode samples were washed, placed into small evaporating dishes that contained 1.5 mL of dimethyl carbonate (DMC), and left for 2 minutes. The samples were then removed from the DMC and allowed to dry in the glove box for less than 5 minutes.

The other half of the electrode samples were not washed. These samples were prepared in the same way and placed into evaporating dishes, but without DMC.

2.2. Characterization

After unwinding and harvesting the electrodes in a glove box, samples were transferred to an adjoining glove box via a common antechamber for analysis using IR and XPS. During this transfer, samples were exposed to pressures around 1.0×10^{-4} kPa for 15 minutes.

Infra-red spectroscopy was performed using a Perkin Elmer Spectrum 100 Fourier-transform, IR spectrometer in attenuated total reflectance mode, using a diamond crystal. A background spectrum was collected prior to data collection. The total force applied to the samples was kept constant.

Scanning electron microscope samples were transferred to the microscope using a custom-made, air-tight sample holder, which was adapted from that used by Howe et al. [13]. Micrographs were collected on a JEOL JSM 6610LV scanning electron microscope using an accelerating voltage of 10 kV and a working distance of 15 mm using a secondary electron detector.

X-ray photoelectron spectroscopy samples (10×10 mm) were mounted on a sample holder by means of double-sided tape. Spectroscopy was performed using a Physical Electronics 5000 VersaProbe II with a monochromatic aluminum Kα (15 kV) X-ray source. The excitation beam size employed was 100 μm and the power was 25 W. Pressures of the system were between 2×10^{-10} kPa before sample insertion and 2×10^{-9} kPa immediately after. Ar^+ ion sputtering was performed at 500 V over an area of 3×3 mm. Spectra were recorded in Fixed Analyzer Transmission mode, using a pass energy value of 11.75 eV, step size of 0.1 eV and acquisition time of 2.7 s/step acquisition time. Binding energy correction was carried out assuming that the main component of the C1s region after sputtering corresponds to C-C (graphite) environments at 284.4 eV, and before sputtering was C-C/C-H environments at 284.8 eV.

3. Results and Discussion

3.1. Morphology

Fig. 1 shows SEM micrographs of the surface of the graphite electrodes harvested from a series of aged $LiCoO_2$/graphite cells with varying contents of VC additive (see *Experimental*). The top row corresponds to unwashed electrodes and the bottom row to electrodes washed in DMC prior to examination.

For the unwashed samples, no surface film was apparent on electrode surface for the cell containing 2% VC; two different surface films were visible on the other samples, depending on the concentration of VC. The first of these was visible with 0 and 1% VC. This film was comprised of individual particles that were 1–5 μm in length and 2 μm in width. Graphite was visible beneath these particles at 1% VC, whereas it wasn't at 0% VC. The particles appeared visually identical in size and structure suggesting that only the quantity of the particles was reduced when 1% of VC was added to the electrolyte. A film with a different structure was visible at the surface of the 4 and 6% VC additive graphite electrodes and it appeared as a solid layer that covered the graphite particles. This covered the grain boundaries in such a way that determining where one particle started and another stopped was not possible. In addition, no constituting particles were observed in the surface film for the 4% and 6% VC content when imaged at the

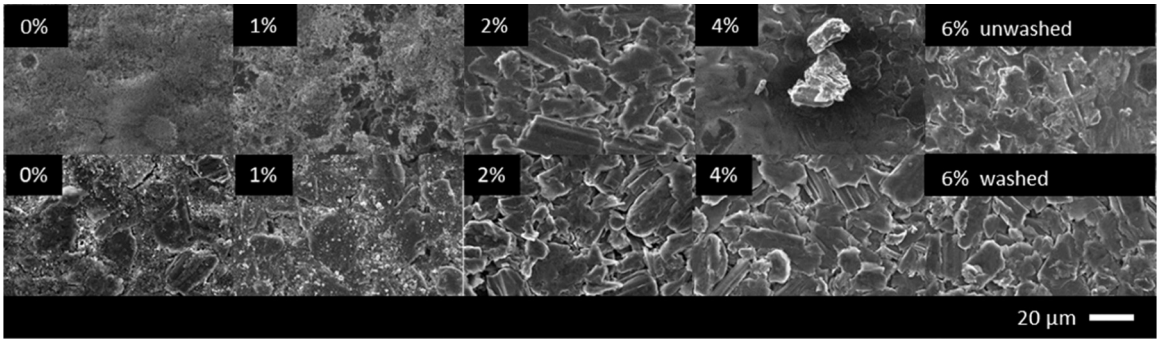

Fig. 1. SEM images of graphite electrodes harvested from $LiCoO_2$/graphite cells with varying concentrations of VC in the electrolyte (concentration indicated in labels). The washed electrodes (bottom row) were immersed in DMC and left to dry prior to analysis; the unwashed electrodes (top row) were simply let dry.

same magnification as the corresponding 0% and 1% VC content samples. Therefore, if the films formed at 4% and 6% VC were composed of particles, they must be much smaller than those constituting the 0 and 1% VC films.

When the electrodes were washed, their visual appearance changed (except for the 2% VC sample, which remained apparently film free). In the case of the 0% electrode, the surface film particles were the same size and shape after washing but had significantly reduced in number so that the underlying graphite particles became visible. The 1% VC washed electrode looked identical to the washed 0% electrode, whereas prior to washing they were different. For the 4 and 6% VC samples, the graphite grain boundaries became distinct and individual graphite particles could be distinguished, showing that the film had been reduced considerably to the point where it was no longer visible. The micrographs of the 2, 4, and 6% VC electrodes after washing appear visually identical.

The main reason given for washing electrodes is to remove salt and/or solvent deposited from the electrolyte during electrode drying. The fact that the morphology of the surface films observed on the unwashed samples is dependent on VC concentration strongly suggests that these films are not simply electrolyte precipitates, which would not be expected to depend on the *initial* concentration of an electrolyte additive consumed on the initial cycles. An alternative hypothesis is that the VC additive is not fully consumed and that the observed differences correspond to changes in (degraded) electrolyte composition. In this case, the morphology of the films corresponding to 0% and 1% VC could be interpreted as precipitates from a degraded electrolyte in cells cycled long enough to consume the protective VC additive; while the clean appearance of the 2% VC sample could be interpreted as indicative of a high enough VC concentration to last the complete aging experiment. However, this scenario would predict the samples with higher VC concentrations to also look clean, which is contradicted by the above observations.

The morphology evolution of the surface films suggests the presence of, at least, two competing SEI forming mechanisms. The first one, which dominates at lower VC concentrations, produces a fine particulate cover and is hindered by VC; as evidenced by the lower coverage of the 1% VC sample compared to the 0% VC sample. The second mechanism, which dominates at higher VC concentrations, produces an apparently dense film and seems to be enhanced by VC; as evidence by its absence on the 2% VC containing sample, and presence at higher VC concentrations. This is supported by the work of Burns et al. [14] who found that the optimum concentration of VC was somewhere between 1 and 2%. They found that charge endpoint slippage reduced at higher concentrations of VC but that at concentrations of 2% and greater cell impedance also increased. Our results show that these two surface films respond differently to electrode washing in DMC. While the washing only partially removes the first, it removes the second completely.

Having established that there are morphological differences between the washed and the unwashed samples, in the following paragraphs we focus on elucidating the differences in chemical composition between these surface films.

3.2. Chemical composition

Fig. 2 shows the IR spectra of both unwashed (a) and washed (b) graphite electrodes. The unwashed IR spectra in Fig. 1 (a) can be separated into three separate groups. The first is 0% VC, containing significant peaks at ~2970 cm^{-1}, 1770 cm^{-1}, and multiple other peaks at less than 1500 cm^{-1}. The second is 1% VC, containing a much smaller peak at 1770 cm^{-1} and multiple broader peaks at less than 1500 cm^{-1}. The final group is electrodes 2, 4, and 6% VC which all have a minor absorption at 1770 cm^{-1} and some broad absorptions in the spectra at less than 1500 cm^{-1}. Overall, the intensity of the absorption bands tends to decrease with increasing concentrations of VC. In particular, the intensity of the carbonyl stretch at ~1770 cm^{-1} decreased by two-orders of magnitude as the concentration of VC increased from 0% to 2%, then remained roughly constant.

Washing the electrodes significantly reduced, or removed completely, each of these peaks. The intensities of the bands from the organics were much weaker after the sample was washed, as shown in Fig. 2 (b). Albeit still present, the bands in the 0% VC sample after washing were much weaker compared to those in the analogous, unwashed sample. For 1% VC the absorption bands are barely visible; and for 2% and above VC concentrations the bands were not visible at all.

These observations are in good qualitative agreement with the aforementioned SEM results, suggesting the formation of two different kinds of films for VC concentrations below and above 2%. The FTIR results also support the hypothesis that the films formed at higher VC concentrations are much more easily washed off by rinsing in DMC than those formed at lower VC concentrations.

As we have previously mentioned, it is assumed that washing removes $LiPF_6$ salt and the low boiling point solvent, which in our case is EC. It is difficult to verify this for the $LiPF_6$ salt using IR

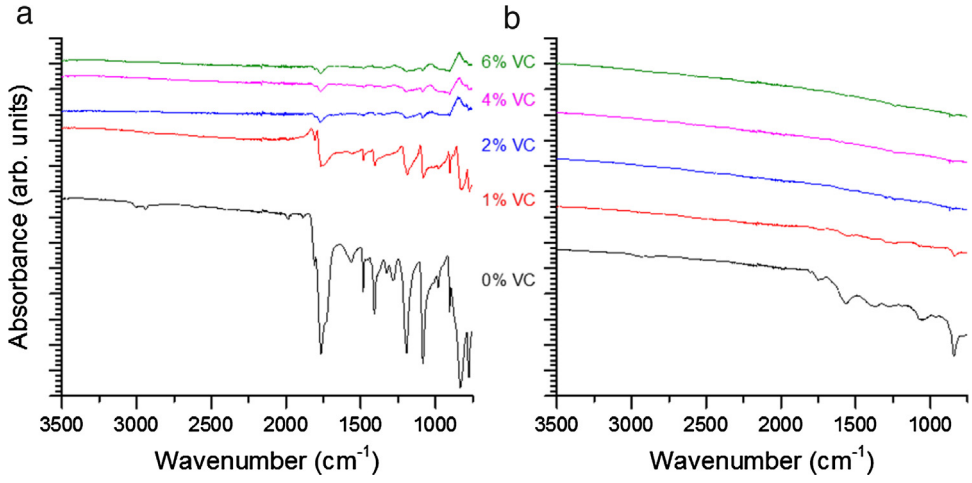

Fig. 2. IR spectra of graphite electrodes with varying percentages of VC additive. The unwashed and washed IR spectra are shown in panels a and b, respectively.

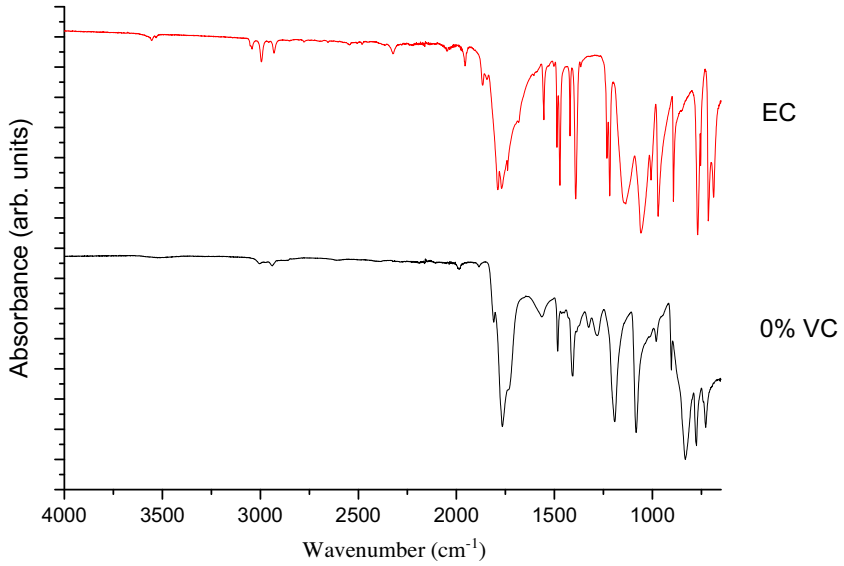

Fig. 3. ATR FT-IR spectrum of solid ethylene carbonate and a graphite electrode from a used lithium-ion cell containing no vinylene carbonate.

because the only IR characteristic peaks occur at 820 and 550 cm^{-1} and this means the position varies considerably with the chemical environment [15]. However, if occurring, EC removal should result in clear IR spectral changes at wavelengths above 1500 cm^{-1}.

Fig. 3 contains an FTIR spectrum of EC next to the corresponding spectrum from the unwashed 0% VC sample. The EC spectrum shows a characteristic triplet of peaks at ~2970 cm^{-1} from the sp^3 hybridized C-H bonds, a strong absorption at ~1770 cm^{-1} from the carbonate ester, and various stretches at wavenumbers below 1500 cm^{-1}. Comparison of the absorbance between EC and 0% VC (Fig. 3) shows that for each stretch in EC there is a corresponding stretch in the 0% VC spectra. This shows that EC is present in the 0% VC sample. However, there are also multiple additional absorbance's for the 0% VC, so there are other components present; but this makes quantitative comparison of absorbance areas difficult. In contrast, there is no corresponding 2970 cm^{-1} triplet of peaks for the 1–6% VC electrodes; showing that there is no EC present (or not at a significant concentration) prior to washing and suggesting that washing is not required to remove it from these samples.

One explanation for the absence of EC is its sublimation dependence on pressure. Fig. 4 contains a plot of data points from the work of Chernyak et al. [16], showing that the sublimation point of EC reduces with pressure. Fitting Chernyak et al. data to $y = a\ln(x) + b$ produced the observed trend line. The values for the fitting coefficients were 34.48 and 85.86, respectively. The regression coefficient, r^2, was 0.99.

Using this equation, the sublimation point of EC at ambient pressure is estimated to be 244.7 °C, lower than the actual boiling point by 16 °C. The calculated sublimation temperature of ethylene carbonate at pressures used in XPS and SEM (1.3×10^{-6} kPa) using this calculation would be below −273.5 °C. Therefore, it can be assumed that EC would be sublimed from the surface of the electrode. Our samples were subjected to low pressures (1.3×10^{-4} kPa) when transferred from the preparation area to the characterization area for IR. The sublimation of EC at this pressure, using the same calculation, is −231 °C. Therefore, after exposure to low pressure, the EC would be expected to sublime sufficiently so that it would not be easily detectable with IR, which supports our results. Therefore, washing is not required to remove EC.

Using the same dataset from previous work by Chernyak et al. [16], we found that propylene carbonate had a sublimation temperature, which was theoretically lower than EC, of approximately −270 °C, at a pressure of 1.0×10^{-4} kPa. This suggests that other commonly used higher boiling point solvents added to battery electrolytes would also sublime at the low pressures found for SEM and XPS analysis and washing is not required to remove them.

The 0% VC electrode has a triplet of peaks at ~2970 cm^{-1} and therefore, EC could be present in this sample. The presence of EC on the surface of the 0% VC sample indicates the limitations in the above calculation. The 0% VC sample's surface film is composed of individual 1–5 μm particles all interlayered on top of the graphite (see Fig. 3). The sublimation rate of EC is dependent on the surface structure. In our case, these interlayered particles create a porous-like material that reduces the rate at which EC sublimes. Because ATR-IR typically has an analysis depth of 2–20 μm it is analyzing well into the surface film material and therefore detecting EC, which has been unable to sublime. This could be overcome by increasing the time under vacuum and/or subjecting the sample to higher vacuums, as is the case in SEM and XPS analysis.

Fig. 5 shows XPS C1s, O1s and F1s data corresponding to unwashed graphite electrodes with varying percentages of VC additive. In agreement with SEM and FTIR results presented above,

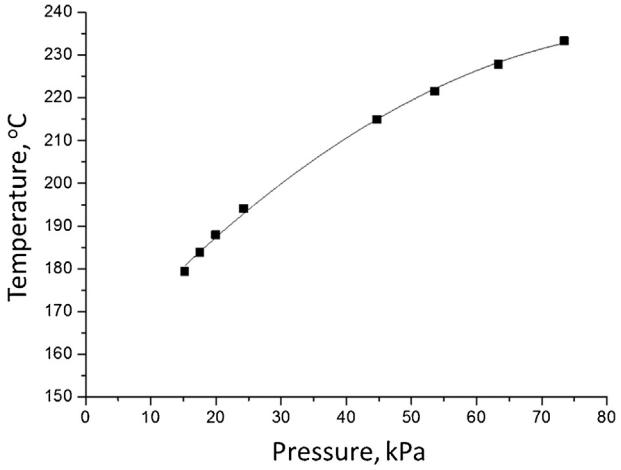

Fig. 4. Plot of sublimation temperature versus pressure for EC taken from the work of Chernyak et al. [13]. The markers represent the data points and the solid curved line, the least-squares fit of the data.

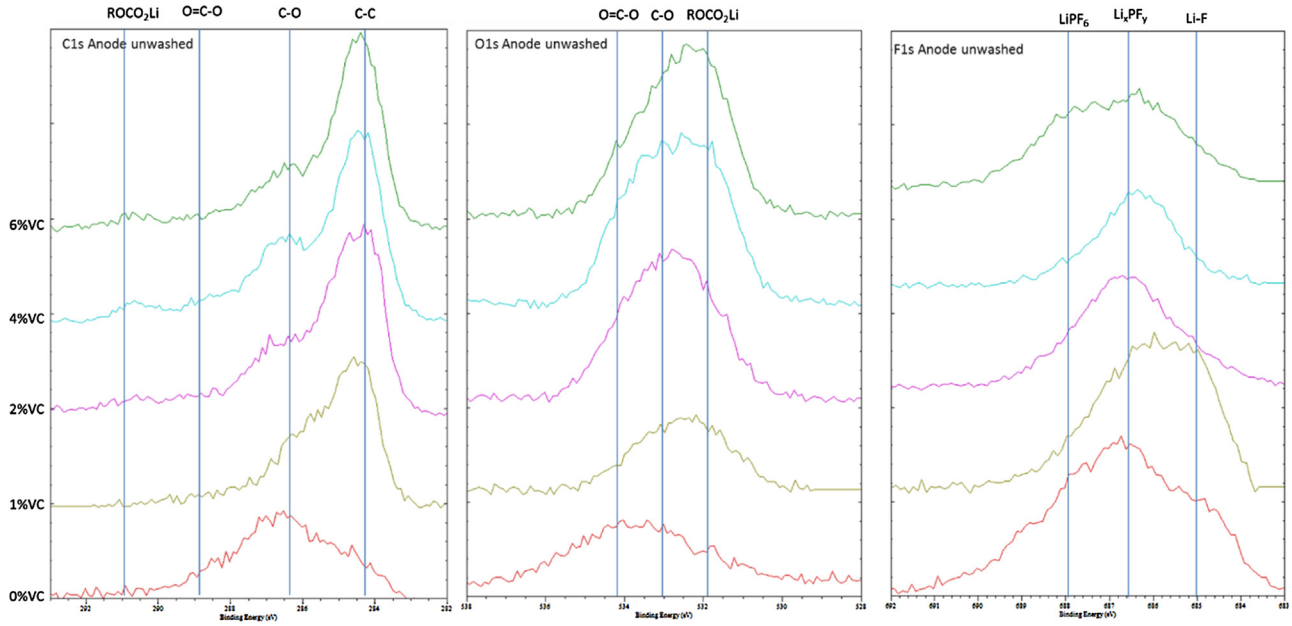

Fig. 5. XPS spectra of the C1s, O1s and F1s regions of unwashed graphite electrode from cells at varying concentrations of VC (0–6%).

there are clear trends in the data following VC concentration. First, the areas of both the C1s and O1s regions seem to increase monotonically with VC content, indicating a higher content of these elements in the surface films formed at higher VC concentrations. Second, in the C1s region there is a clear contribution of C-C environments around 284.4 eV in the samples with 1% and higher VC content. The C1s region of the 0% VC sample is dominated by an ether-like C-O-C contribution around 286.5 eV. Although there is no clearly resolved C-C peak in the 0% VC sample, there is still significant intensity around 284.5 eV. Finally, for 4% and 6% VC content, there is appreciable contribution from $ROCO_2Li$ [17] functionalities around 291 eV.

Third, the trends in peak positions for the F1s and O1s regions are less clear. The O1s region corresponding to the 0%VC sample is centered on 534 eV, suggesting a dominance of ether-like C-O-C environments. Starting at 1% VC the O1s region shifts to lower B.E. around 532 eV, suggesting the emergence of carbonate-like CO_3 functionality. As the VC content increases, both C-O-C and CO_3 contributions increase. Meanwhile, the overall F1s intensity seems to decrease with VC content, with low VC samples showing a higher contribution of LiF-like functionality around 685–686 eV. The 2% and 4% VC samples present narrower F1s regions centered around 687 eV, where the 0% and 1% VC samples also present significant intensity. The overall trend is masked by the presence of strong $LiPF_6$-like contributions around 688 eV in both the 0% and 6% VC samples.

Overall, the XPS data series presented in Fig. 5 is consistent with the formation of different films at VC concentrations above and below 2%. Turning our attention to salt contributions from the data, it has to be recognized that precipitates from the drying electrolyte (e.g. $LiPF_6$) could be masking the surface films and confusing the trends in the XPS data above. This is, in essence, the rationale for washing the samples. However, the disappearance of high VC content surface film signatures from SEM and FTIR data above counsels caution. In the following paragraphs, we explore Ar^+ sputtering as an alternative route to remove these precipitates for XPS analysis.

Fig. 6 shows F1s XPS spectra of the washed and unwashed anodes harvested from the cell containing 1% VC, both before and after 1 min. Ar^+ ion-sputtering. After 1 min. of sputtering time the sample reaches steady state and the shape of the F1s regions does not change with further sputtering time. The spectra are deconvoluted by least square fitting using GL(30) (i.e., 30% Gaussian) peak shapes in CasaXPS. Washed electrodes are well described with one component centered at ~686.5 eV, suggesting the presence of a single chemical environment, while three components are necessary to describe unwashed electrodes. Unwashed electrodes require two additional components to be described, centered at ~685 and ~688 eV. The component centered on ~686.5 eV, which was present for both washed and unwashed electrodes, can be attributed to Li_xPF_y. chemical environments; while the components centered at ~685 and ~688 eV can be attributed to LiF and $LiPF_6$ chemical environments, respectively [18].

The F1s XPS spectrum of the unwashed electrode prior to sputtering is dominated by the Li_xPF_y component, which accounts for approximately 70% of the total area, while the LiF and $LiPF_6$ contributions account for approximately 25% and 5% of the region area, respectively. Following the work of Ensling et al., [18] we attribute the $LiPF_6$ and Li_xPF_y contributions to salt precipitates resulting from electrolyte evaporation during sample harvesting. After sputtering, the $LiPF_6$ contribution remains approximately constant, while the area of the Li_xPF_y contribution is reduced by half and the area of the LiF contribution is doubled. The sputtering process removes most of the salt deposits from the surface. However, the combination of sampling area (~200 μm spot diameter) and the high surface roughness (~μm) with respect to sputtering depth ($\lesssim$100 nm) makes it very unlikely that these precipitates will be completely removed from the sample by the sputtering process. I.e., salt precipitates between particles will be screened from the Ar^+ beam and will contribute some signal even when, at steady state, most of the XPS signal comes from the layer underneath them. Therefore, the increase in absolute intensity of the LiF signal is consistent with LiF being present in the SEI at higher contents than in the precipitate layer. This observation, together with the fact that LiF is not a component of the electrolyte, strongly suggest that LiF forms during the cycling process and is incorporated into the SEI.

In contrast, the washed film showed only the Li_xPF_y component; which remains the only component in the washed electrode after

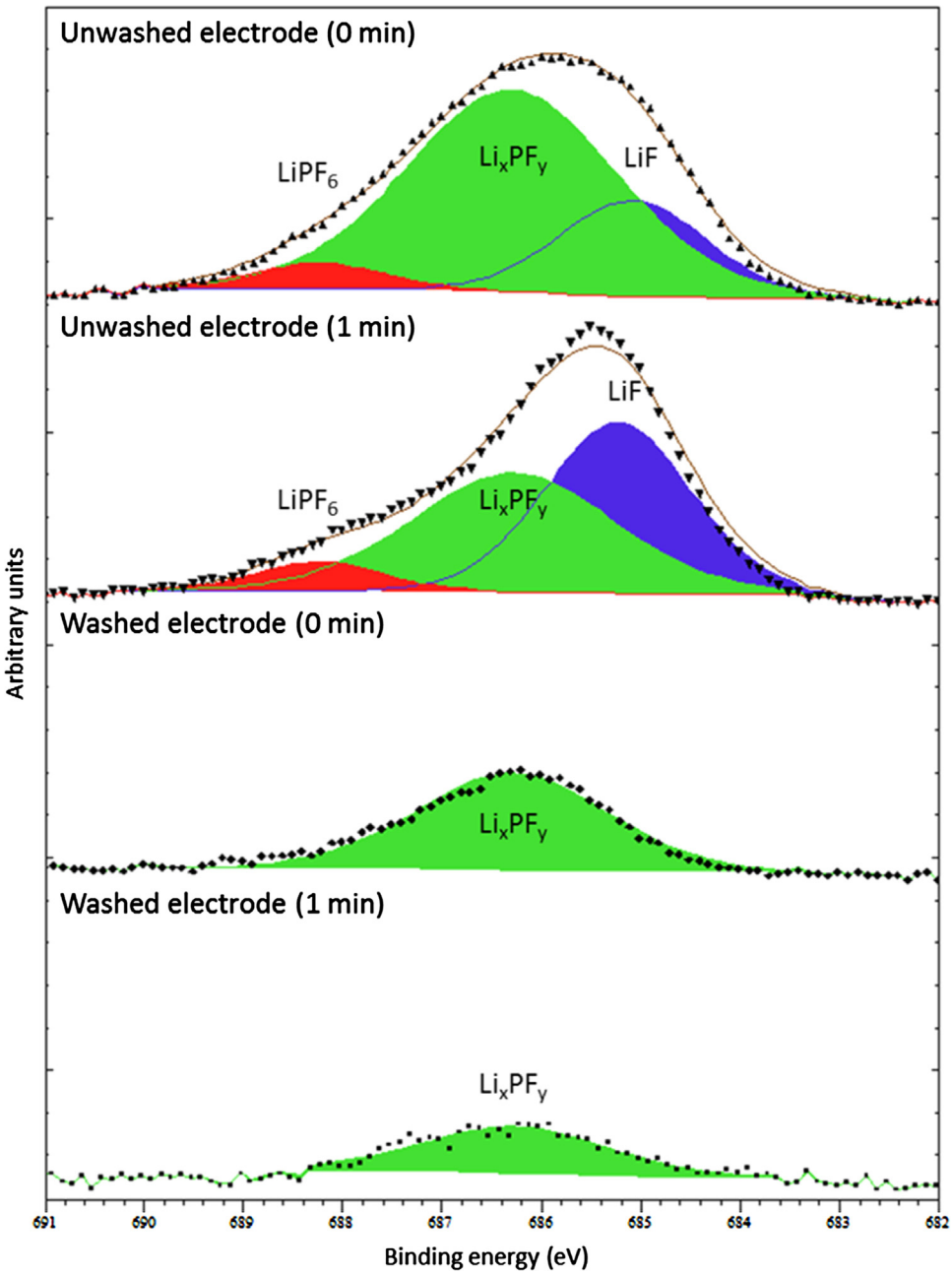

Fig. 6. F1s XPS results from the washed and unwashed samples. 0 min represents unsputtered electrodes, whereas 1 min represents the sample after sputtering. The peaks represent different chemical environments based on the expected fluorine environments in the sample.

sputtering, albeit with reduced intensity. Furthermore, its binding energy and peak width are not affected by the sputtering process. The absence of LiF and $LiPF_6$ signatures in the washed electrodes is consistent with previous reports [19] that DMC washing is an efficient way of removing salt deposits from graphite electrodes. Our results indicate that DMC washing removes LiF functionalities from deeper strata of the SEI, which are revealed by Ar^+ sputtering in the corresponding unwashed sample.

In an operating cell, one would expect reaction products to deposit on the electrode surface. If these products were partly soluble in the electrolyte, deposition will occur only after the products reach saturation in the electrolyte.

In the cell, there is a small amount of electrolyte which can dissolve these materials; typically, the amount of electrolyte is a few times the pore volume in the electrodes. Thus, only a small amount of SEI material would be expected to be in solution in the cell. Given that we used 1.5 mL of DMC to wash the electrode samples, it is very possible that the washing solvent may remove orders of magnitude more SEI materials than would be found in the electrolyte at saturation. The point here is that it does not matter if we used DMC or DEC for the washing process. Both have the potential for removing SEI. Until the exact nature of the SEI is known, the extent of material removal will have to be judged based on experiments like this one.

It should be noted that electrode surfaces before and after sputtering are inhomogeneous, stochastically ordered complex mixtures of unknown precise composition. Sputtering can move, rearrange and bury SEI components in such materials. By ensuring that the XPS detection area was large (~100 μm diameter), it should be a representative cross section of the electrode surface and militate against pockets or isolated regions causing bias in the results. To ensure this was the case during the sputtering process,

samples were sputtered for 30 seconds, interleaved with XPS analysis. This continued until the spectra didn't change between sputtering. As suggested by Steinberger et al. [20], we also used low Ar^+ ion energy and additional analytical methods to mitigate any potential bias. However, further work is required to systematically assess the impact of sputtering on lithium-ion surface films.

4. Conclusion

In summary, consistent with previous reports, we observed two different films on aged graphite anodes harvested from LCO/electrolyte/VC/graphite cells. The first kind is dominant at VC concentrations below 2%, appears granular in SEM images, has strong organic signals in FTIR and its growth appears to be inhibited by VC. The second kind is dominant at VC concentrations above 2%, appears smooth in SEM images and does not present strong organic signals in FTIR.

Micrographs and FTIR spectra show that washing graphite electrodes with DMC for one and a half minutes is sufficient to remove the film that forms at greater than 2%, and greatly reduce the film present at less than 2%. XPS analysis suggests that, contrary to expectations, the effects of DMC washing on the first film are not confined to removal of extraneous salt deposits from the electrolyte, but also remove LiF and Li_xPF_y components of deeper layers of the SEI structure.

Acknowledgements

We acknowledge support from the Engineering and Physical Sciences Research Council (EPSRC) and the WMG centre HVM Catapult. We also acknowledge support from Jaguar Land Rover Automotive PLC.

The work at Argonne National Laboratory was performed under the auspices of the U.S. Department of Energy (DOE), Office of Vehicle Technologies (VTO), under Contract No. DE-AC02-06CH11357.

The submitted issue has been created by the University of Chicago as Operator of Argonne National Laboratory ("Argonne") under Contract No. W-31-109-Eng-38 with the U.S. Department of Energy. The U.S. Government retains for itself, and others acting on its behalf, a paid-up, non-exclusive, irrevocable, worldwide license in said article to reproduce, prepare derivative works, distribute copies to the public, and perform publicly and display publicly, by or on behalf of the Government.

References

[1] J.-M. Tarascon, M. Armand, Issues and challenges facing rechargeable lithium batteries, Nature 414 (6861) (2001) 359–367.
[2] S.B. Peterson, J. Apt, J. Whitacre, Lithium-ion battery cell degradation resulting from realistic vehicle and vehicle-to-grid utilization, Journal of Power Sources 195 (8) (2010) 2385–2392.
[3] M. Lu, H. Cheng, Y. Yang, A comparison of solid electrolyte interphase (SEI) on the artificial graphite anode of the aged and cycled commercial lithium ion cells, Electrochimica Acta 53 (9) (2008) 3539–3546.
[4] L. Yang, B. Ravdel, B.L. Lucht, Electrolyte reactions with the surface of high voltage LiNi0. 5Mn1. 5O4 cathodes for lithium-ion batteries, Electrochemical and Solid-State Letters 13 (8) (2010) A95–A97.
[5] E. Peled, The electrochemical behavior of alkali and alkaline earth metals in nonaqueous battery systems—the solid electrolyte interphase model, Journal of The Electrochemical Society 126 (12) (1979) 2047–2051.
[6] P. Arora, R.E. White, M. Doyle, Capacity fade mechanisms and side reactions in lithium-ion batteries, Journal of the Electrochemical Society 145 (10) (1998) 3647–3667.
[7] C.K. Chan, R. Ruffo, S.S. Hong, Y. Cui, Surface chemistry and morphology of the solid electrolyte interphase on silicon nanowire lithium-ion battery anodes, Journal of Power Sources 189 (2) (2009) 1132–1140.
[8] R. Dedryvère, S. Laruelle, S. Grugeon, L. Gireaud, J.-M. Tarascon, D. Gonbeau, XPS identification of the organic and inorganic components of the electrode/electrolyte interface formed on a metallic cathode, Journal of The Electrochemical Society 152 (4) (2005) A689–A696.
[9] S. Malmgren, K. Ciosek, R. Lindblad, S. Plogmaker, J. Kühn, H. Rensmo, K. Edström, M. Hahlin, Consequences of air exposure on the lithiated graphite SEI, Electrochimica Acta 105 (2013) 83–91.
[10] N. Williard, B. Sood, M. Osterman, M. Pecht, Disassembly methodology for conducting failure analysis on lithium–ion batteries, Journal of Materials Science: Materials in Electronics 22 (10) (2011) 1616–1630.
[11] F. Orsini, A. Du Pasquier, B. Beaudoin, J. Tarascon, M. Trentin, N. Langenhuizen, E. De Beer, P. Notten, In situ scanning electron microscopy (SEM) observation of interfaces within plastic lithium batteries, Journal of power sources 76 (1) (1998) 19–29.
[12] L. Chen, K. Wang, X. Xie, J. Xie, Effect of vinylene carbonate (VC) as electrolyte additive on electrochemical performance of Si film anode for lithium ion batteries, Journal of Power Sources 174 (2) (2007) 538–543.
[13] J.Y. Howe, L.A. Boatner, J.A. Kolopus, L.R. Walker, C. Liang, N.J. Dudney, C.R. Schaich, Vacuum-tight sample transfer stage for a scanning electron microscopic study of stabilized lithium metal particles, Journal of Materials Science 47 (3) (2012) 1572–1577.
[14] J. Burns, R. Petibon, K. Nelson, N. Sinha, A. Kassam, B. Way, J. Dahn, Studies of the effect of varying vinylene carbonate (VC) content in lithium ion cells on cycling performance and cell impedance, Journal of The Electrochemical Society 160 (10) (2013) A1668–A1674.
[15] J.-W. Liu, X.-H. Li, Z.-X. Wang, H.-J. Guo, W.-J. Peng, Y.-H. Zhang, Q.-Y. Hu, Preparation and characterization of lithium hexafluorophosphate for lithium-ion battery electrolyte, Transactions of Nonferrous Metals Society of China 20 (2) (2010) 344–348.
[16] Y. Chernyak, J.H. Clements, Vapor pressure and liquid heat capacity of alkylene carbonates, Journal of Chemical & Engineering Data 49 (5) (2004) 1180–1184.
[17] D. Aurbach, B. Markovsky, I. Weissman, E. Levi, Y. Ein-Eli, On the correlation between surface chemistry and performance of graphite negative electrodes for Li ion batteries, Electrochimica acta 45 (1) (1999) 67–86.
[18] D. Ensling, M. Stjerndahl, A. Nytén, T. Gustafsson, J.O. Thomas, A comparative XPS surface study of Li 2 FeSiO 4/C cycled with LiTFSI-and LiPF 6-based electrolytes, Journal of Materials Chemistry 19 (1) (2009) 82–88.
[19] K. Tasaki, A. Goldberg, J.-J. Lian, M. Walker, A. Timmons, S.J. Harris, Solubility of lithium salts formed on the lithium-ion battery negative electrode surface in organic solvents, Journal of The Electrochemical Society 156 (12) (2009) A1019–A1027.
[20] R. Steinberger, J. Walter, T. Greunz, J. Duchoslav, M. Arndt, S. Molodtsov, D. Meyer, D. Stifter, XPS study of the effects of long-term Ar+ ion and Ar cluster sputtering on the chemical degradation of hydrozincite and iron oxide, Corrosion Science 99 (2015) 66–75.